M&C 2017 - International Conference on Mathematics & Computational Methods Applied to Nuclear Science & Engineering, Jeju, Korea, April 16-20, 2017, on USB (2017)

Improved Two-Level p-CMFD Acceleration in Neutron Transport Calculation

Seungsu Yuk and Nam Zin Cho*

Korea Advanced Institute of Science and Technology (KAIST)
291 Daehak-ro, Yuseong-gu, Daejeon, Korea 34141
**Corresponding Author: nzcho@kaist.ac.kr*

Abstract - *This work verifies the cause of slow convergence for optically thick coarse mesh cell sizes when coarse mesh based acceleration is applied to the neutron transport criticality calculation. To overcome the limitation, the present paper introduces two two-level iterative schemes to speedup coarse mesh based acceleration. In the schemes, a fine mesh based acceleration with the fixed source is augmented in a coarse mesh based acceleration with the fission source. These techniques are applied to the partial current-based coarse mesh finite difference (p-CMFD) method, that is a more stable acceleration method than other coarse mesh based acceleration methods. Simple analyses of numerical problems show that the techniques enhance the convergence speed of p-CMFD, especially for optically thick coarse mesh cells.*

I. INTRODUCTION

To reduce the computational burden in neutron transport calculation, various acceleration methods have been developed [1]. Among them, coarse mesh based acceleration methods [2–8] are widely used, because they are easily applied to the original transport calculation with various geometries. However, a drawback of coarse mesh based acceleration methods is that they exhibit slow convergence or divergent behavior for optically thick coarse mesh cells. This drawback limits the size of coarse mesh cells. In eigenvalue problems, they incur non-negligible computational burden per iteration.

The present paper investigates the cause of such slow convergence or divergent behavior. To overcome the limitation, two two-level iterative schemes are introduced in this paper to speedup coarse mesh based acceleration. These techniques are applied to the partial current-based coarse mesh finite difference (p-CMFD) method [5–8], that is a more stable acceleration method than other coarse mesh based acceleration methods. Simple analyses of numerical problems show that the techniques enhance the convergence speed of p-CMFD, especially for optically thick coarse mesh cells.

II. COARSE MESH BASED ACCELERATION

This section discusses the nonlinear acceleration methods currently in use, especially the p-CMFD method.

1. Coarse Mesh Based Acceleration

Coarse mesh based acceleration methods usually consist of two parts: a high-order calculation and a low-order calculation. The high-order calculation employs transport methods with fixed fission source. The low-order calculation uses the balance equation, in which the high-order calculation provides parameters over each coarse mesh cell. The low-order calculation gives the multiplication factor and the coarse mesh cell averaged scalar flux. The coarse mesh cell averaged scalar fluxes are then "modulated" to be used in the fission source of the high-order equation for the next iteration.

2. Description of p-CMFD Acceleration

The p-CMFD acceleration is a modification of the CMFD acceleration, in that p-CMFD is based on the use of partial currents instead of net currents used in CMFD, resulting in i) p-CMFD is unconditionally stable and ii) p-CMFD provides additional information, that is transport partial currents (instead of net current) on the interface of two coarse mesh cells. This subsection presents the formula of p-CMFD acceleration.

Let us first consider a neutron transport equation. For the sake of simplicity, steady-state one-dimensional planar problem with one-group, isotropic scattering is considered. The discrete ordinate transport sweep procedure with single scattering source iteration is as follows:

$$\frac{\mu_n}{h_k}(\psi_{n,k+1/2}^{(l+1/2)}-\psi_{n,k-1/2}^{(l+1/2)})+\sigma_{t,k}\psi_{n,k}^{(l+1/2)} = \sigma_{s,k}\phi_k^{(l)}+\frac{1}{k_{eff}^{(l)}}\nu\sigma_{f,k}\phi_k^{(l)}, \tag{1}$$

$$\psi_{n,1/2}^{(l+1/2)}=\alpha_L\psi_{N+1-n,1/2}^{(l+1/2)},\ \mu_n>0, \tag{2}$$

$$\psi_{n,K+1/2}^{(l+1/2)}=\alpha_R\psi_{N+1-n,K+1/2}^{(l+1/2)},\ \mu_n<0, \tag{3}$$

$$\psi_{n,k}^{(l+1/2)}=\frac{1+\beta_{n,k}}{2}\psi_{n,k+1/2}^{(l+1/2)}+\frac{1-\beta_{n,k}}{2}\psi_{n,k-1/2}^{(l+1/2)}, \tag{4}$$

$$\beta_{n,k}=\begin{cases}0 & \text{for DD,}\\ \coth(\sigma_{t,k}h_k/\mu_n)-\dfrac{2\mu_n}{\sigma_{t,k}h_k} & \text{for SC,}\end{cases} \tag{5}$$

$$\phi_k^{(l+1/2)}=\frac{1}{2}\sum_{n=1}^{N}w_n\psi_{n,k}^{(l+1/2)}, \tag{6}$$

where $1 \le n \le N$, $1 \le k \le K$ are the indices of discretized angles and fine mesh cells, respectively, DD means the diamond difference scheme, and SC means the step characteristic scheme. The remaining notations are standard.

The p-CMFD equation is obtained after the transport sweep. The coarse mesh surface partial currents are obtained as:

$$J_{j+1/2,+}^{(l+1/2)} = \frac{1}{2}\sum_{\mu_n>0} w_n |\mu_n| \psi_{n,k+1/2}^{(l+1/2)}, \quad (7)$$

$$J_{j+1/2,-}^{(l+1/2)} = \frac{1}{2}\sum_{\mu_n<0} w_n |\mu_n| \psi_{n,k+1/2}^{(l+1/2)}, \quad (8)$$

where $0 \le j \le J$, $j+1/2$ is an index for surfaces of coarse mesh cells, $k+1/2$ is an index for surfaces of fine mesh cells satisfying that fine mesh cell k belongs to coarse mesh cell j and fine mesh cell $k+1$ belongs to coarse mesh cell $j+1$ ($k \in j$, $k+1 \in j+1$). The coarse mesh averaged flux is also obtained as:

$$\overline{\phi}_j^{(l+1/2)} = \frac{1}{\Delta_j}\sum_{k\in j} \phi_k^{(l+1/2)} h_k, \quad (9)$$

where $1 \le j \le J$, j is an index for coarse mesh cells and Δ_j is the size of coarse mesh cell j. The coarse mesh homogenized cross sections are also defined as:

$$\overline{\sigma}_{t,j}^{(l+1/2)} = \frac{1}{\overline{\phi}_j^{(l+1/2)}\Delta_j}\sum_{k\in j} \sigma_{t,k}\phi_k^{(l+1/2)} h_k, \quad (10)$$

$$\overline{\sigma}_{s,j}^{(l+1/2)} = \frac{1}{\overline{\phi}_j^{(l+1/2)}\Delta_j}\sum_{k\in j} \sigma_{s,k}\phi_k^{(l+1/2)} h_k, \quad (11)$$

$$\overline{\nu\sigma}_{f,j}^{(l+1/2)} = \frac{1}{\overline{\phi}_j^{(l+1/2)}\Delta_j}\sum_{k\in j} \nu\sigma_{f,k}\phi_k^{(l+1/2)} h_k. \quad (12)$$

At the surface $j+1/2$ between coarse-mesh cells j and $j+1$, the outgoing and incoming partial currents are related with the corresponding cell-averaged scalar fluxes, respectively, as:

$$\begin{aligned} J_{j+1/2,+}^{(l+1/2)} &= -(1/2)\tilde{D}_{j+1/2}^{(l+1/2)}(\overline{\phi}_{j+1}^{(l+1/2)} - \overline{\phi}_j^{(l+1/2)}) \\ &\quad + \hat{D}_{j+1/2,+}^{(l+1/2)}\overline{\phi}_j^{(l+1/2)}, \end{aligned} \quad (13)$$

$$\begin{aligned} J_{j+1/2,-}^{(l+1/2)} &= (1/2)\tilde{D}_{j+1/2}^{(l+1/2)}(\overline{\phi}_{j+1}^{(l+1/2)} - \overline{\phi}_j^{(l+1/2)}) \\ &\quad + \hat{D}_{j+1/2,-}^{(l+1/2)}\overline{\phi}_{j+1}^{(l+1/2)}, \end{aligned} \quad (14)$$

where $\tilde{D}_{j+1/2}^{(l+1/2)}$ is an arbitrary constant (usually chosen as the coupling coefficient determined in the ordinary finite difference method). Two correction factors are defined to preserve the respective partial currents as:

$$\hat{D}_{j+1/2,+}^{(l+1/2)} = \frac{J_{j+1/2,+}^{(l+1/2)} + (1/2)\tilde{D}_{j+1/2}^{(l+1/2)}(\overline{\phi}_{j+1}^{(l+1/2)} - \overline{\phi}_j^{(l+1/2)})}{\overline{\phi}_j^{(l+1/2)}}, \quad (15)$$

$$\hat{D}_{j+1/2,-}^{(l+1/2)} = \frac{J_{j+1/2,-}^{(l+1/2)} - (1/2)\tilde{D}_{j+1/2}^{(l+1/2)}(\overline{\phi}_{j+1}^{(l+1/2)} - \overline{\phi}_j^{(l+1/2)})}{\overline{\phi}_{j+1}^{(l+1/2)}}. \quad (16)$$

CMFD uses one correction coefficient to preserve the surface net current. On the other hand, p-CMFD uses two correction coefficients to preserve the surface partial currents. The surface net current is automatically preserved by the two surface partial currents.

By substituting the above equations into the neutron balance equation over each coarse mesh cell, the result is a finite difference form of low-order diffusion-type equation called p-CMFD equation, that can be easily solved:

$$\begin{aligned} &J_{j+1/2}^{(l+1)} - J_{j-1/2}^{(l+1)} + (\overline{\sigma}_{t,j}^{(l+1/2)} - \overline{\sigma}_{s,j}^{(l+1/2)})\overline{\phi}_j^{(l+1)}\Delta_j \\ &\qquad = \frac{1}{k_{eff}^{(l+1)}}\overline{\nu\sigma}_{f,j}^{(l+1/2)}\overline{\phi}_j^{(l+1)}\Delta_j, \end{aligned} \quad (17)$$

$$\begin{aligned} J_{j+1/2}^{(l+1)} &= -\tilde{D}_{j+1/2}^{(l+1/2)}(\overline{\phi}_{j+1}^{(l+1)} - \overline{\phi}_j^{(l+1)}) \\ &\quad - (\hat{D}_{j+1/2,-}^{(l+1/2)}\overline{\phi}_{j+1}^{(l+1)} - \hat{D}_{j+1/2,+}^{(l+1/2)}\overline{\phi}_j^{(l+1)}). \end{aligned} \quad (18)$$

The solution of Eqs. (17)–(18) is then "modulated" to be used in the right hand side of Eq. (1) for the next iteration:

$$\phi_k^{(l+1)} = \phi_k^{(l+1/2)} \cdot \frac{\overline{\phi}_j^{(l+1)}}{\overline{\phi}_j^{(l+1/2)}}, \; 1 \le k \le K, \; k \in j. \quad (19)$$

The above p-CMFD equations can be described in symbolic expression as:

High-order equation: $M\psi^{(l+1/2)} = \frac{1}{k_{eff}^{(l)}} F\phi^{(l)}$, (20)

Low-order equation: $\overline{M}^{(l+1/2)}\overline{\phi}^{(l+1)} = \frac{1}{k_{eff}^{(l+1)}}\overline{F}^{(l+1/2)}\overline{\phi}^{(l+1)}$, (21)

Prolongation: $\phi^{(l+1)} = I\left(\phi^{(l+1/2)}, \overline{\phi}^{(l+1)}\right)$. (22)

III. LIMITATIONS OF COARSE MESH BASED ACCELERATION

This section discusses the stability of coarse mesh based acceleration methods, the $\tilde{D}$ optimized p-CMFD, and the limitations of coarse mesh based acceleration methods.

1. Fourier Stability Analysis of Coarse Mesh Based Accelerations

To study the efficiency of such an acceleration, Fourier convergence analysis was performed on coarse mesh rebalance (CMR) [4,8], coarse mesh finite difference (CMFD) [8,9], and p-CMFD [5–9]. Figure 1 shows that p-CMFD is always stable and more stable than the other methods. In Figure 1, the number of fine mesh cells in a coarse mesh cell, called granularity, is set to 20. CMR shows divergent behavior for optically thin coarse mesh cells. p-CMFD and CMFD are efficient for optically thin coarse mesh cells but not efficient for optically thick coarse mesh cells. (CMFD even diverges for optically thick coarse mesh cells).

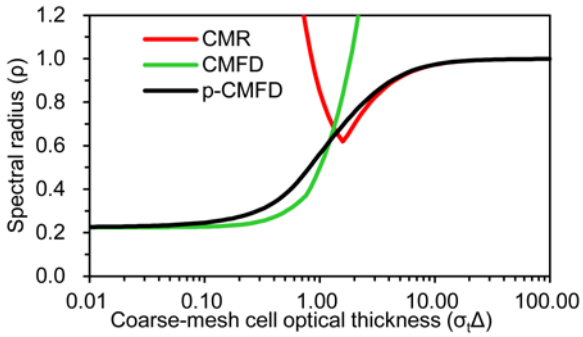

Fig. 1. Results of Fourier stability analysis of CMR, CMFD, and p-CMFD with SC and S_{16} for the eigenvalue problem (number of scattering iterations = 1, granularity = 20).

2. Optimization of Diffusion Coefficient

CMFD and p-CMFD use the diffusion coefficient $\tilde{D}$ which comes from the standard diffusion theory. (The results of spectral radius designated as p-CMFD throughout the figures in this paper are those of "standard" p-CMFD). In theory, the diffusion coefficient can be chosen arbitrarily. Refs. 10 and 11 adjusted the diffusion coefficient in CMFD to improve the convergence speed. Ref. 12 used a modified parameter related to the diffusion coefficient in the nonlinear diffusion acceleration (NDA) so that the acceleration was stabilized. We adjust the diffusion coefficient $\tilde{D}$ in p-CMFD to optimize the spectral radius. The golden section search method is used to find the optimized diffusion coefficient. Figure 2 shows that the $\tilde{D}$ optimized p-CMFD leads to a slightly reduced spectral radius.

3. Lower Bound of the Rate of Convergence

Even with the optimizing $\tilde{D}$, p-CMFD shows slow convergence in optically thick coarse mesh cells. This is a common property for all coarse mesh based acceleration methods; see Ref. 11. It comes from the disagreement between the coarse-mesh level convergence and the fine-mesh level convergence. In the sense of error reduction, there are errors which cannot be reduced by coarse-mesh based low-order calculation (these errors are not zeros in fine-mesh level, although the average value over each coarse mesh cell is zero). Thus, the reduction rate of these errors depends only on the high-order transport calculation. These errors give the lower limit of the spectral radius for coarse mesh based accelerations.

Figure 2 displays the theoretical lower bound of coarse mesh based acceleration methods and the spectral radius of the fine mesh limit with the optimizing diffusion coefficient $\tilde{D}$. Optimized p-CMFD is very close to the fine mesh limit for optically thin coarse mesh cells and to the lower bound for optically thick coarse mesh cells. Optimized CMFD obtained in Ref. 11 is also shown in Fig. 2. Both methods with optimized $\tilde{D}$ improve the convergence rates in optically thin coarse mesh cells, that are already very fast. However, because the lower bound of the spectral radius of coarse mesh based acceleration methods is close to unity for optically thick coarse mesh cells, any coarse mesh based acceleration method will exhibit slow convergence for optically thick coarse mesh cells.

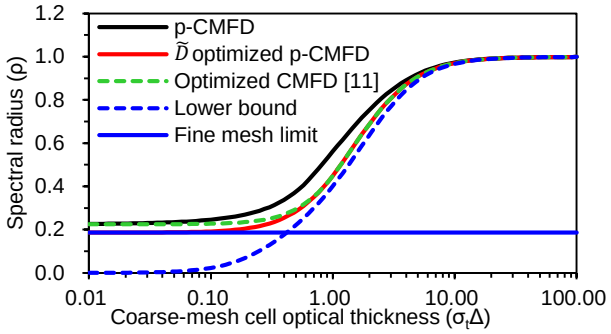

Fig. 2. Spectral radius of the $\tilde{D}$ optimized p-CMFD and the lower bound of coarse mesh based acceleration.

IV. TWO-LEVEL p-CMFD ACCELERATIONS

To overcome the limitations of coarse mesh based acceleration methods, we should reduce the corresponding errors which cannot be reduced by coarse mesh based calculation. This section describes two-level p-CMFD techniques to speedup p-CMFD acceleration, particularly in optically thick coarse mesh cells. A simple one-dimensional problem (1000 cm, homogeneous problem with vacuum boundary condition on both ends) is used to test the efficiency of the techniques. The computational conditions are as follows: Fine mesh size is 0.01 cm, granularity is 100, and S_{16} calculations with the step characteristic scheme are performed. We change the value of the total cross section to estimate the spectral radius for any coarse mesh optical thickness.

1. p-FMFD Augmented Two-Level p-CMFD

This subsection describes the procedure of p-FMFD augmented two-level p-CMFD. Let us consider a partial current-based fine mesh finite difference acceleration with fixed fission source (denoted as p-FMFD) before or after p-CMFD eigenvalue calculation.

To describe the p-FMFD equation, we start from the transport sweep:

$$M\psi^{(l+1/4)} = \frac{1}{k_{eff}^{(l)}} F\phi^{(l)}. \tag{23}$$

Before the usual p-CMFD eigenvalue equation, we construct a p-FMFD equation, which is a p-CMFD type equation on each fine mesh cells with fixed fission source:

$$J_{k+1/2,+}^{(l+1/4)} = \frac{1}{2}\sum_{\mu_n>0} w_n |\mu_n| \psi_{n,k+1/2}^{(l+1/4)}, \tag{24}$$

$$J_{k+1/2,-}^{(l+1/4)} = \frac{1}{2}\sum_{\mu_n<0} w_n |\mu_n| \psi_{n,k+1/2}^{(l+1/4)}, \tag{25}$$

$$\begin{aligned} J_{k+1/2,+}^{(l+1/4)} &= -(1/2)\tilde{D}_{k+1/2}^{(l+1/4)}(\phi_{k+1}^{(l+1/4)} - \phi_k^{(l+1/4)}) \\ &\quad + \hat{D}_{k+1/2,+}^{(l+1/4)}\phi_k^{(l+1/4)}, \end{aligned} \tag{26}$$

$$\begin{aligned} J_{k+1/2,-}^{(l+1/4)} &= (1/2)\tilde{D}_{k+1/2}^{(l+1/4)}(\phi_{k+1}^{(l+1/4)} - \phi_k^{(l+1/4)}) \\ &\quad + \hat{D}_{k+1/2,-}^{(l+1/4)}\phi_{k+1}^{(l+1/4)}, \end{aligned} \tag{27}$$

$$\hat{D}_{k+1/2,+}^{(l+1/4)} = \frac{J_{k+1/2,+}^{(l+1/4)} + (1/2)\tilde{D}_{k+1/2}^{(l+1/4)}(\phi_{k+1}^{(l+1/4)} - \phi_k^{(l+1/4)})}{\phi_k^{(l+1/4)}}, \tag{28}$$

$$\hat{D}_{k+1/2,-}^{(l+1/4)} = \frac{J_{k+1/2,-}^{(l+1/4)} - (1/2)\tilde{D}_{k+1/2}^{(l+1/4)}(\phi_{k+1}^{(l+1/4)} - \phi_k^{(l+1/4)})}{\bar{\phi}_{k+1}^{(l+1/4)}}, \tag{29}$$

$$\begin{aligned} &J_{k+1/2}^{(l+2/4)} - J_{k-1/2}^{(l+2/4)} + (\sigma_{t,k} - \sigma_{s,k})\phi_k^{(l+2/4)} h_k \\ &= \frac{1}{k_{eff}^{(l)}} \nu\sigma_{f,k}\phi_k^{(l)} h_k, \end{aligned} \tag{30}$$

$$\begin{aligned} J_{k+1/2}^{(l+2/4)} &= -\tilde{D}_{k+1/2}^{(l+1/4)}(\phi_{k+1}^{(l+2/4)} - \phi_k^{(l+2/4)}) \\ &\quad -(\hat{D}_{k+1/2,-}^{(l+1/4)}\phi_{k+1}^{(l+2/4)} - \hat{D}_{k+1/2,+}^{(l+2/4)}\phi_k^{(l+2/4)}). \end{aligned} \tag{31}$$

There is no spatial homogenization to construct p-FMFD equation. Compared to the usual p-CMFD acceleration, p-FMFD with fixed fission source incurs small additional computational burden. When the p-FMFD calculation is performed before the p-CMFD eigenvalue calculation, whole-core p-FMFD calculation is used for the stability.

After whole-core p-FMFD calculation, the usual p-CMFD is computed using the result of whole-core p-FMFD:

$$\bar{M}^{(l+2/4)}\bar{\phi}^{(l+3/4)} = \frac{1}{k_{eff}^{(l+3/4)}} \bar{F}^{(l+2/4)}\bar{\phi}^{(l+3/4)}, \tag{32}$$

$$\phi^{(l+3/4)} = I\left(\phi^{(l+2/4)}, \bar{\phi}^{(l+3/4)}\right). \tag{33}$$

After whole-core p-CMFD eigenvalue calculation, p-FMFD can be performed under the updated fission source:

$$\begin{aligned} &J_{k+1/2}^{(l+1)} - J_{k-1/2}^{(l+1)} + (\sigma_{t,k} - \sigma_{s,k})\phi_k^{(l+1)} h_k \\ &= \frac{1}{k_{eff}^{(l+3/4)}} \nu\sigma_{f,k}\phi_k^{(l+3/4)} h_k, \end{aligned} \tag{34}$$

$$\begin{aligned} J_{k+1/2}^{(l+1)} &= -\tilde{D}_{k+1/2}^{(l+3/4)}(\phi_{k+1}^{(l+1)} - \phi_k^{(l+1)}) \\ &\quad -(\hat{D}_{k+1/2,-}^{(l+3/4)}\phi_{k+1}^{(l+1)} - \hat{D}_{k+1/2,+}^{(l+3/4)}\phi_k^{(l+1)}), \end{aligned} \tag{35}$$

$$k_{eff}^{(l+1)} = k_{eff}^{(l+3/4)}, \tag{36}$$

where the two-correction factors are computed as in the previous whole-core p-FMFD.

When the p-FMFD calculation is performed after the p-CMFD calculation, local p-FMFD calculations over coarse mesh cells are used. Each p-FMFD calculation over a coarse mesh cell is performed independently of p-FMFD calculations over other coarse mesh cells. To set up the boundary conditions for each p-FMFD, the incoming partial currents are necessary, and that is why we use the p-CMFD framework, which provides the transport corrected partial currents:

$$J_{j-1/2}^{(l+1)} = J_{j-1/2,+}^{(l+3/4)} - \frac{J_{j-1/2,-}^{(l+3/4)}}{\phi_k^{(l+3/4)}}\phi_k^{(l+1)},\ k \in j,\ k-1 \in j-1, \tag{37}$$

$$J_{j+1/2}^{(l+1)} = \frac{J_{j-1/2,+}^{(l+3/4)}}{\phi_k^{(l+3/4)}}\phi_k^{(l+1)} - J_{j+1/2,-}^{(l+3/4)},\ k \in j,\ k+1 \in j+1. \tag{38}$$

Figure 3 compares the p-FMFD augmented two-level p-CMFD techniques with the usual p-CMFD. Note that the spectral radii of two-level p-CMFD accelerations are smaller than the lower bound for optically thick coarse mesh cells in Figure 2. Three cases show similar convergence rates.

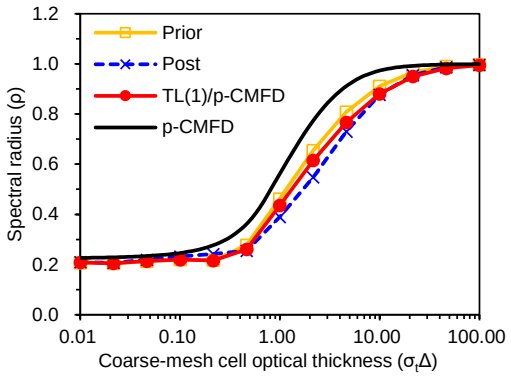

Fig. 3. Spectral radius of two-level p-CMFD augmented with p-FMFD (Prior: p-FMFD before p-CMFD calculation, Post: p-FMFD after p-CMFD calculation, TL(1)/p-CMFD: one p-FMFD before and after p-CMFD calculation).

2. Local/Global Iterations in Two-Level p-CMFD

Even though we add p-FMFD procedures, it still gives slow convergence for optically thick coarse mesh cells. To reduce the spectral radius further, we introduce the local/global iterative framework to the low-order calculation in a two-level p-CMFD. Figure 4 is the flow chart of such a two-level p-CMFD. Modifying the p-FMFD doubly augmented two-level p-CMFD in the previous subsection, a local/global iteration procedure is introduced between the whole-core p-CMFD eigenvalue calculation and the local p-FMFD fixed fission source calculations.

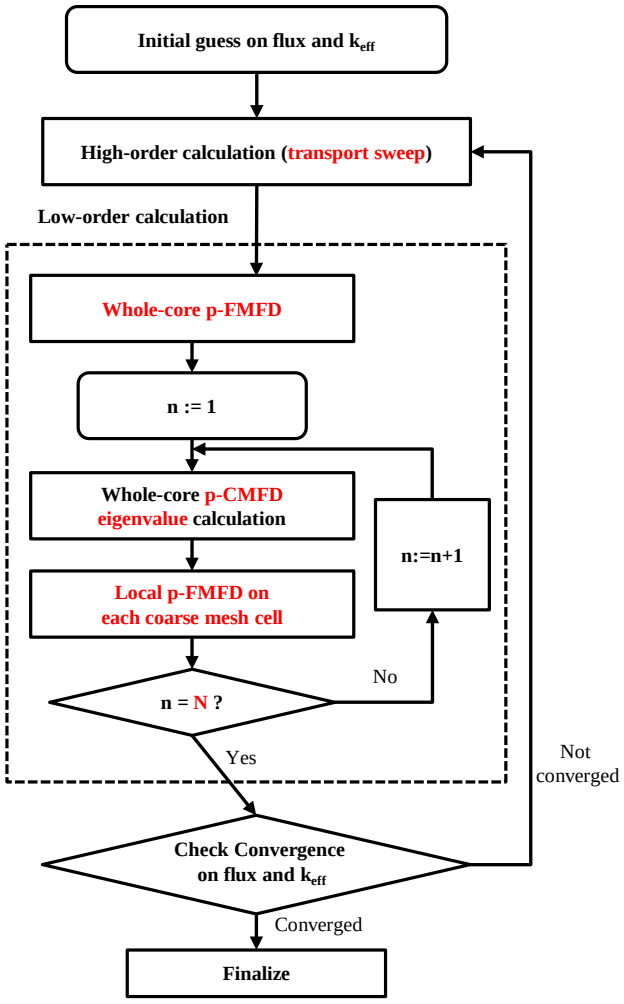

Fig. 4. Flow chart of local/global iterative framework in two-level p-CMFD.

Figure 5 is the result of local/global iterations in a two-level p-CMFD. As the number of local/global iterations increases, the spectral radius for optically thick coarse mesh cells reduces drastically approaching that of fine mesh limit.

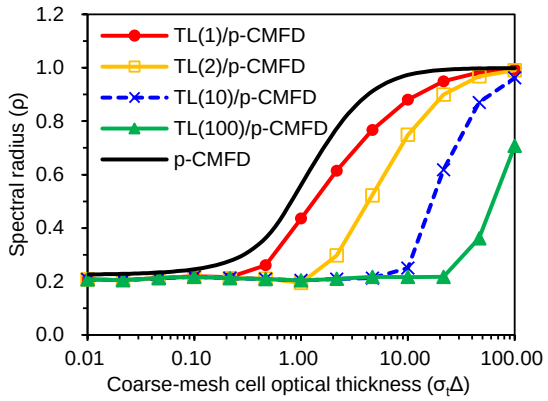

Fig. 5. Spectral radius of local/global iteration in a two-level p-CMFD (TL(N)/p-CMFD: a two-level p-CMFD with N local/global iterations).

V. NUMERICAL RESULTS

To test the two-level p-CMFD for a heterogeneous problem, the following test problem is considered. The test problem is a modified C5G7 OECD/NEA benchmark problem [13] with 17 assemblies, which is shown in Figure 6.

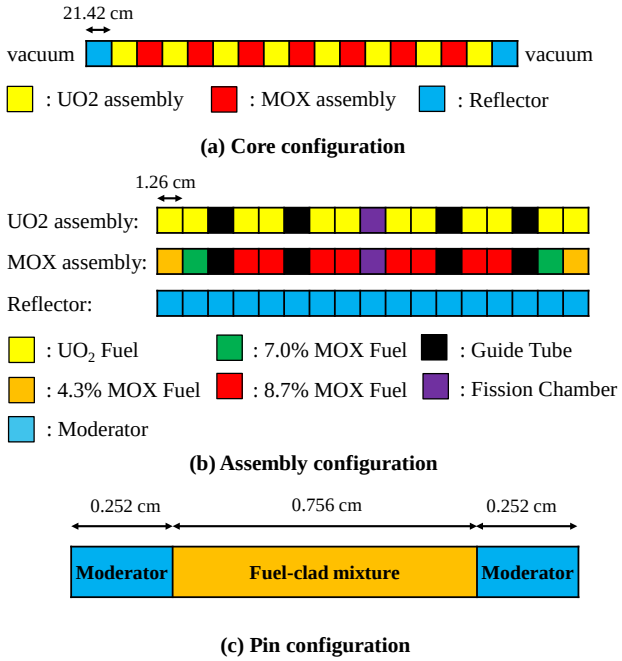

Fig. 6. Geometry of test problem.

This problem is a one-dimensional problem with the seven-group cross section data that are specified in the C5G7 benchmark report [13]. The computational conditions

are as follows: Fine mesh size is 0.042 cm, and S_{32} calculations with the diamond difference scheme are performed. Each assembly forms a coarse mesh cell in p-CMFD calculation. Error criteria are 10^{-7} for maximum relative error of neutron flux and multiplication factor. We perform the usual p-CMFD and two-level p-CMFD calculations to test the computing efficiency.

Table I shows the computing performance of usual p-CMFD and two-level p-CMFD acceleration methods. All methods give the same multiplication factor as expected. Note that the usual p-CMFD with assembly coarse mesh cell size reduces the number of iterations in S_N calculation. But it still requires hundreds of iterations to converge. Two-level p-CMFD reduces the number of iterations further: TL(1)/p-CMFD is about 11 times faster than the usual p-CMFD. TL(4)/p-CMFD is about 2 times faster than TL(1)/p-CMFD.

Figure 7 shows the calculation times for various granularity values. When the p-CMFD with one granularity is used, calculation time exceeds 10.0 sec, the top of the range shown in Figure 7. Note that the usual p-CMFD achieves the best computing performance for half-pin coarse mesh cell size. But the efficiency of the usual p-CMFD drops dramatically when the sizes of coarse mesh cells are far from the optimal case. On the other hand, two-level p-CMFD calculations show the best computing performance for sub-assembly or assembly sizes of coarse mesh cells. Moreover, the calculation in two-level p-CMFD is less sensitive to the granularity than that in the usual p-CMFD.

Table I. Computing performance on test problem of Fig. 6

	No Acc	p-CMFD	TL(1)/ p-CMFD	TL(4)/ p-CMFD
k_{eff}	1.25846	1.25846	1.25846	1.25846
Number of iterations	6050	743	53	15
Transport calculation time (sec)[a]	152.18	18.90	1.49	0.44
Acceleration calculation time (sec)[a]	0	4.28	0.62	0.61
Total calculation time (sec)	153.13	23.30	2.11	1.06
Speedup	1	6.57	72.57	144.46

[a] Computation with a single thread of a CPU (Intel Core i7-3770K)

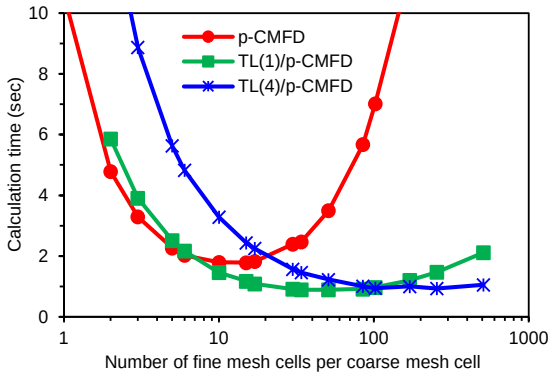

Fig. 7. Calculation times for various granularity values in p-CMFD.

VI. CONCLUSIONS

This paper presents the speedup techniques for p-CMFD acceleration in neutron transport calculation. We introduce two techniques that are more effective than the optimized p-CMFD (with optimized diffusion coefficient) for optically thick coarse mesh cells. In the first technique, the p-FMFD with the fixed source is augmented in a usual p-CMFD with the fission source. The spectral radius of the first technique is smaller than the lower bound of spectral radius of coarse mesh based acceleration methods. However, the first technique is still slow for optically thick coarse mesh cells.

To improve this situation, we also consider the local/global iterations of local p-FMFD and global p-CMFD. The results of this second technique show that we obtain fast convergence (even for large coarse-mesh cells) if we use a sufficient number of local/global iterations. Hence, it has the potential to overcome the limitation of coarse mesh based acceleration.

There are some problems still remaining for future work. For example, the number of local/global iterations should be controlled adaptively to reduce the unnecessary waste of computational time. The application and performance of the techniques to two-dimensional and three-dimensional realistic problems remain to be studied.

REFERENCES

1. M. L. ADAMS and E. W. LARSEN, "Fast Iterative Methods for Discrete-Ordinates Particle Transport Calculations," *Prog. Nucl. Energy*, **40**, 3 (2002).
2. E. E. LEWIS and W. F. MILLER, Jr., *Computational Methods of Neutron Transport*, John Wiley & Sons, New York (1984).
3. K. S. SMITH and J. D. RHODES III, "Full-Core, 2-D, LWR Core Calculations with CASMO-4E," *Proc.*

PHYSOR 2002, Seoul, Korea, October 7–10, 2002, American Nuclear Society (2002) (CD-ROM).

4. G. R. CEFUS and E. W. LARSEN, "Stability Analysis of Coarse-Mesh Rebalance," *Nucl. Sci. Eng.*, **105**, 31 (1990).
5. N. Z. CHO, G. S. LEE, and C. J. PARK, "On a New Acceleration Method for 3D Whole-Core Transport Calculations," *Annual Mtg. Atomic Energy Society of Japan*, Sasebo, Japan, March 27–29, 2003, Atomic Energy Society of Japan (2003).
6. N. Z. CHO, G. S. LEE, and C. J. PARK, "Partial Current-Based CMFD Acceleration of the 2D/1D Fusion method for 3D Whole-Core Transport Calculations," *Trans. Am. Nucl. Soc.*, **88**, 594 (2003).
7. N. Z. CHO, "The Partial Current-Based CMFD (p-CMFD) Method Revisited," *Trans. Kor. Nucl. Soc.*, Gyeongju, Korea, October 25–26, 2012, Korean Nuclear Society (2012).
8. N. Z. CHO and C. J. PARK, "A Comparison of Coarse Mesh Rebalance and Coarse Mesh Finite Difference Accelerations for the Neutron Transport Calculations," *Proc. M&C 2003*, Gatlinburg, Tennessee, April 6–11, 2003, American Nuclear Society (2003); see also KAIST internal report NURAPT-2002-02, (with addendum on p-CMFD), http://nurapt.kaist.ac.kr/lab/report/NurapT2002_2rev2.pdf
9. S. G. HONG, K. S. KIM, and J. S. SONG, "Fourier Convergence Analysis of the Rebalance Methods for Discrete Ordinates Transport Equations in Eigenvalue Problems," *Nucl. Sci. Eng.*, **164**, 33 (2010).
10. A. YAMAMOTO, "Generalized Coarse-Mesh Rebalance Method for Acceleration of Neutron Transport Calculations," *Nucl. Sci. Eng.*, **151**, 274 (2005).
11. A. ZHU, M. JARRETT, Y. XU, B. KOCHUNAS, E. W. LARSEN, and T. DOWNAR, "An Optimally Diffusive Coarse Mesh Finite Difference Method to Accelerate Neutron Transport Calculations," *Ann. Nucl. Energy*, **95**, 116 (2016).
12. S. SCHUNERT, Y. WANG, J. ORTENSI, F. GLEICHER, B. BAKER, M. DEHART, and R. MARTINEAU, "A Flexible Nonlinear Diffusion Acceleration Method for the First Order Eigenvalue S_N Equations Discretized with Discontinuous FEM," *Proc. PHYSOR 2016*, Sun Valley, Idaho, May 1–5, 2016, American Nuclear Society (2016).
13. M. A. SMITH, E. E. LEWIS, and B.-C. NA, "Benchmark on Deterministic Transport Calculations Without Spatial Homogenization: A 2-D/3-D MOX Fuel Assembly 3-D Benchmark," NEA/NSC/DOC(2003)16, Organisation for Economic Co-operation and Development, Nuclear Energy Agency (2003).